Optical and organic vapor properties of Calix[4]arene based macrocyclic Langmuir-Blodgett thin films

Y. ACIKBAS[a,*], N. ZEYBEK[a], C. OZKAYA[b], A. SIRIT[c], M. ERDOGAN[b], R. CAPAN[b], S. BOZKURT[d,e]
aDepartment of Material Science and Nanotechnology Engineering, Faculty of Engineering, University of Usak, Turkey
bDepartment of Physics, Faculty of Science, University of Balikesir, Turkey
cDepartment of Chemistry, Necmettin Erbakan University, 42099, Meram, Konya, Turkey
dVocational School of Health Services, Usak University, 64200 Usak, Turkey
eScientific Analysis Technological Application and Research Center, Usak University, 64200 Usak, Turkey

Surface Plasmon Resonance (SPR) optical chemical sensors based on 25,27-Bis(N-[[(2R)-2-hydroxy-3-[[(1R)-1-(hydroxymethyl)propyl]amino]propyl]asetamide))-26,28-dihydroxy-5,11,17,23-tetra(tert-butyl)calix[4]arene (NHDACx) films were fabricated to sense dichloromethane, acetone, and benzene at room temperature. Calix[4]arene based macrocyclic thin films, as gas sensing film, were fabricated by Langmuir-Blodgett (LB) thin film technique with different thicknesses, and characterized by SPR and UV-Visible spectrophotometer. The experimental SPR data were fitted using the Winspall software to evaluate optical properties of the NHDACx film such as the parameter of thickness and refractive index. Values of the thickness and refractive index of NHDACx LB films were determined as 1.29 ± 0.06 nm for the thickness per monolayer, and 1.54 ± 0.07 for the refractive index. Exposed to above mentioned organic vapors, the responses of the optical sensors, ΔI, were measured. Optical sensor with 7.9 nm NHDACx film shows higher response to the saturated concentration of all vapors than the others, due to the amount of the adsorbed vapor molecules onto the surface of NHDACx film. Sensing mechanisms are based on changing photodetector response and optical properties of the gas sensing element. As a result, NHDACx optical LB thin film sensors exhibits high response, a good sensitivity and selectivity for saturated dichloromethane vapor than other vapors. These optical thin film sensors were potential candidates for organic vapor sensing applications with simple and low cost preparation at room temperature.

1. Introduction

Some natural or artificial products (paints, varnishes, cleaning, disinfecting, cosmetic, pesticide, stored fuels and automotive products, office equipments etc) as a solid or liquid can release volatile organic compounds (VOCs) into the air. These VOCs may have short- and long-term adverse health effects or some environmental problems in the nature. The ability of VOCs to cause health effects depend on level of exposure and length of time exposed. Reports [1, 2] proved that the immediate symptoms that some people have experienced soon after exposure to some organics include allergic skin reaction, eye and respiratory tract irritation, headaches, dizziness, visual disorders, nose and throat discomfort, fatigue and memory impairment. In the long term they can also cause cancer in human. For the minimizing of VOCs damages on our health it is important to detect the amount of VOCs in our daily life using a highly sensitive and selective VOC sensor.

Today the interests of macrocycle molecules are significantly increasing because they are key materials not only tools for studying molecular recognition, but are also key components for drug delivery [3], clinical development and human treatment [4], environmental chemical sensing applications [5]. The use of macrocycle molecules in the field of sensing applications have several advantages due to their unique cavity-size and cyclization structural organization for host-guest interaction, binding affinity and selectivity (engage specific targets through numerous and spatially distributed binding interactions) [6, 7]. Some important macrocycle molecules used for sensing applications can be given as porphyrins, cyclodextrins, crown ethers and calix[n]arenes. The simple shape of calixresorcinarenes or calix[n]arene molecules is that of a cup with a defined upper and lower rim and a central annulus and allows studying the host-guest interaction for sensor applications as a consequence of their preformed cavities. Either the upper and/or lower rims can be easliy modified adding several different molecular groups to investigate the sensor interaction mechanism. Calix[n]arenes are extensive usage as receptors for cations, anions and even neutral molecules. Incorporation of binding capabilities and chemical groups that respond to analytes complexation has given these macrocycles additional advantages in applications as efficient selective chemical sensors. Therefore macrocycle calix[n]arene molecules have been extensively studied for several sensing applications for host-guest [8,9], hydrogen bonding [10], dipole-dipole [11], π-π interaction [12,13] mechanisms. In our previous studies, pillar[5]arene-quinoline and calix[4]arene molecules prepared as LB thin

film sensing elements were studied extensively for optical detection using SPR technique [14,15]. Both researches showed that they have a high sensitivity and selectivity responses toward particular chemical classes of VOC molecules. In addition, macrocycle calix[4]resorcinarene molecule is suitable for the fabrication of a chemical sensing element with a precise controlled film thickness using the LB thin film deposition technique onto a solid substrate. The multilayer LB film arrangement for a chemical sensing element has a hydrophilic group on its external face and a hydrophobic group on the internal side. The active site, the hydrophilic surface of the calix[4]arene molecule in the open form, interacts with vapor molecules due to strong hydrogen bonds. At the same time, the cavity of the calix[4]arene can provide an advantage for the binding of organic guest molecular species and the sensitivity and selectivity of calix[4]arene.

In this study, Bozkurt et al. [16] synthesized a new chiral calix[4]arene macrocycle bearing amino alcohol moieties at the lower rim from the reaction of p-tert-butylcalix[4]arene diester with amino alcohol group. The multilayer LB film arrangement for a chemical sensing element has a hydrophilic group (-OH) on its external face and a hydrophobic group ($–C(CH_3)_3$) on the internal side. This new material given in Fig. 1 is called as NHDACx. Using this chiral calix[4]arene derivative bearing both an amino group and a hydroxyl group, the first time ultrathin LB film will be prepared as a vapor sensing element. The interaction between calix[4]arene LB film as a host structure and organic vapor as a guest molecule will be investigated for dichloromethane, benzene and acetone vapors.

2. Experimental details

2.1. Preparation of NHDACx LB thin film

Fig. 1 presents the chemical structure of NHDACx molecule which is selected LB thin film materials. The details of synthesis process and characterization of this material is reported by Bozkurt et al. [16]. 2.38 mg mL^{-1} concentration of NHDACx and chloroform solution was smoothly spread on cleaned pure water to investigate the behavior of NHDACx molecules at the air–water interface by taking π-A isotherm graphs. The obtaining of π-A isotherm and the fabrication of NHDACx LB thin films achieved *via* LB through (Model 622-NIMA). A temperature control unit and the microbalance sensor were fixed to this through for controlling the temperature of pure water and surface pressure, respectively. The process of the taking π-A isotherm was started after chloroform had allowed to evaporate for 15-20 minutes. After this stage, the π-A isotherm of NHDACx was taken by compressing (the compression speed of 20 cm^{2}min^{-1}) the monolayer very slowly. The Y type (the selected deposition type) NHDACx LB thin films were prepared at a surface pressure of 28 mN m^{-1}, and this suitable value was determined from the isotherm graph. All NHDACx LB thin film fabrication process was fixed at room temperature.
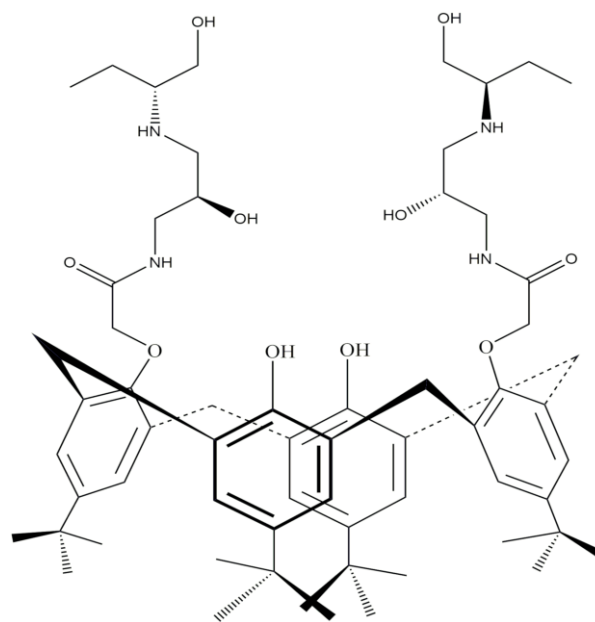

Fig. 1. Chemical structure of NHDACx molecule

2.2. UV-visible spectroscopy analyses

The NHDACx/chloroform solution and the reproducibility of NHDACx LB films deposited onto quartz glass were characterized by UV-Visible spectrophotometer (scanned between the wavelength regions of 190 nm to 900 nm). All UV-Vis results were obtained at fixed absorbance mode of this spectrophotometer which has deuterium-tungsten light source.

2.3. SPR measurement technique

BIOSUPLAR 6 Model Surface Plasmon Resonance Spectrometer was preferred to carry out all SPR measurements and the angular resolution of the SPR measurement was determined as 0.003°. As a light source, a laser diode at a wavelength of 632.8 nm was performed for these measurements. A glass prism of reflective index 1.62 was installed to holder to take measurements in air environment, and 50 nm gold layer coated glass slides were used for all SPR measurements. In order to obtain SPR kinetic measurements, a semi-transparent plastic flow cell was fixed. Thanks to the channels of inlets and outlets, the silicon tubes can be fastened to the cell. The SPR system settings, the data acquiring, and data presentation were controlled by software. The photodetector response was obtained as a function of time by using three different modes (slope mode, tracking mode or single measurements). Differences between these modes can be seen simultaneously via software interface. All kinetic measurements were actualized by exposure fresh air and organic vapor for periodically 2 minutes. In this work, the fitting of experimental SPR curves was fixed with WINSPALL software. The thickness and refractive index values of NHDACx LB thin film can be calculated

through these fitting data. The SPR measurement system as a schematic diagram was presented in Fig. 2.
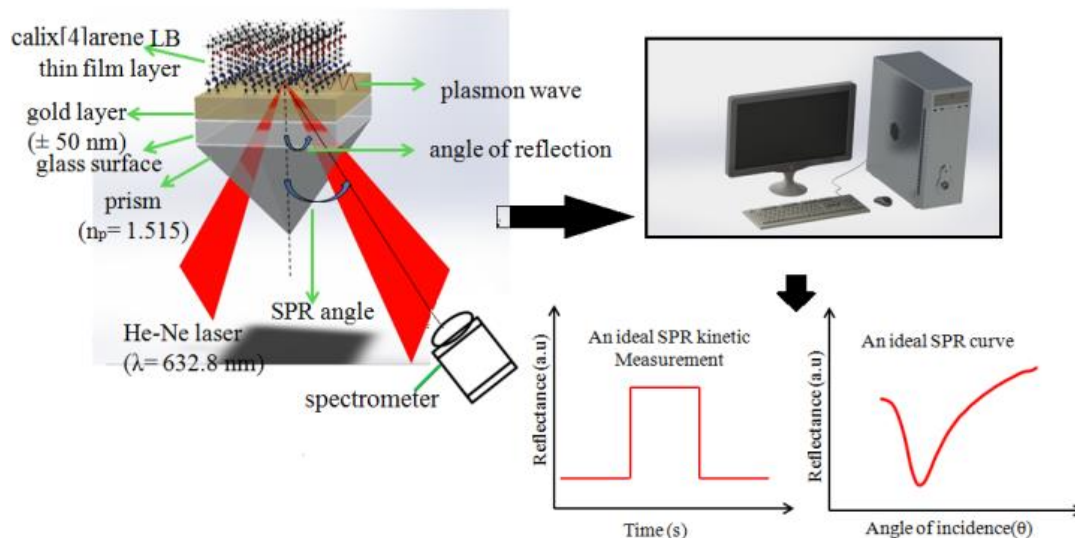

Fig. 2. A shematic diagram of the surface plasmon resonance measurement system (color online)

3. Result and discussion

3.1. NHDACx LB thin film preparation results

The measurement of surface pressure as a function of surface area in the NHDACx monolayer films is known as π-A isotherm characteristics. Π-A isotherm graph of NHDACx monolayer films was taken for two important purposes before NHDACx LB thin films were prepared. The first one to obtain useful information about the NHDACx monolayer films at the air-water interface. The second purpose was for determining a suitable surface pressure value to fabricate homogenous LB thin film. The π-A isotherm for the NHDACx monolayer is shown in Fig. 3. From this graph, a surface pressure of 28 mN m^{-1} was chosen for preparing NHDACx LB films.

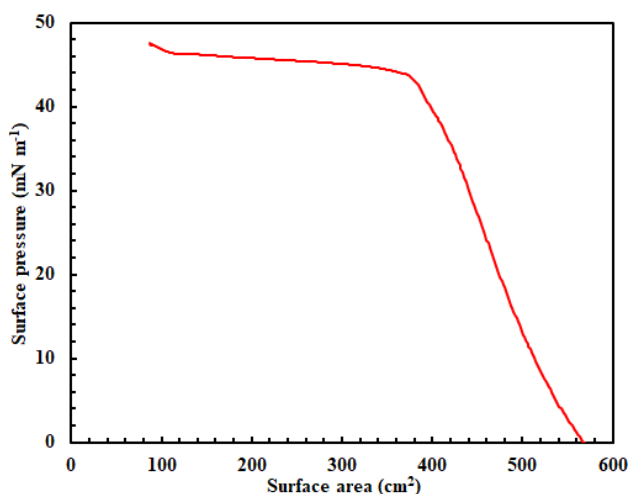*Fig. 3. π-A isotherm graph of NHDACx LB thin film (color online)*

NHDACx LB thin films were prepared onto both quartz glass and gold-coated glass substrates using LB deposition process of Y-type. The surface pressure (28 mN m^{-1}) fixed stable by utilizing the movable barrier (under the certain deposition conditions) to obtain the deposition graph of NHDACx monolayer film from surface to solid substrate up to ten layers (Fig. 4). This graph displays that the monolayer was deposited successfully by calculation of the transfer ratio [17]. It can be estimated that NHDACx is a preferable monomer for the fabrication of homogenous LB thin films from the high value (calculated as ≥ 93%) of transfer ratio.
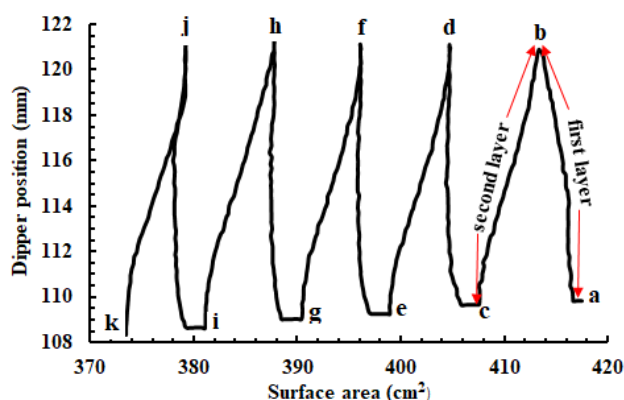

Fig. 4. Transfer graph of NHDACx monolayer on gold-coated glass (color online)

3.2 SPR and UV-visible results

The SPR technique ensures supporting information about the deposition process of NHDACx LB thin films as well as SPR kinetic gas measurements. The change of

reflected light intensity according to the resonance angle shift for 50 nm thick gold coated glass substrate and NHDACx LB thin films at different layers (2, 6, and 10 layers) was displayed in Fig. 5. From this graph, it can be seen that the SPR minimum changed to a greater angle by increasing the number of NHDACx LB film layers. The inset in Fig. 5 presents a linear relationship between the angle shift of NHDACx LB thin films and the number of layers. This relationship indicates that almost equal NHDACx molecules are transferred to the gold-coated glass during NHDACx LB thin film deposition process.
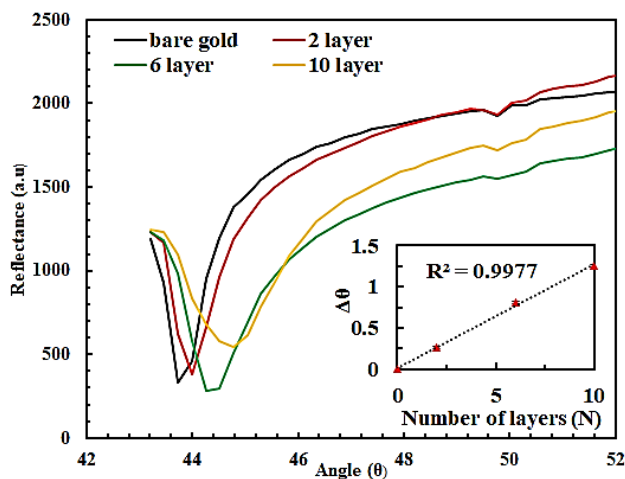

Fig. 5. SPR curves of NHDACx LB films with increase in thickness. Inset:Llinear increase of thickness as a function of number of bilayers (color online)

The affirmation of the fabricated homogeneous NHDACx LB thin film onto quartz glasses was carried out *via* UV-Vis Spectroscopy. Two absorption spectrums of NHDACx / chloroform solution were observed nearly at 215 nm and 260 nm. UV-Vis results for this solution were performed at different concentrations (a= 50 μl, b= 100 μl, c= 150 μl, d= 200 μl, e= 250 μl, f= 300 μl and, g= 350 μl), and shown in Fig. 6. The UV-Vis results of distinct layers of NHDACx LB films on quartz glass substrates for 2, 6, and 10 layers were obtained, and given in the inset-A of Fig. 6. The absorption spectrums were observed approximately at 255 nm for different NHDACx LB layers. The UV-vis spectra of the NHDACx LB films are similar to the solution spectra but the band at 260 nm is broadened in the solution spectrum and is blue shifted by about 5 nm. The shift in the absorption band of the NHDACx LB film may be the result of some kind of molecular aggregation occurring during the film formation[18]. The linearship between absorbance and the number of NHDACx layers was also displayed in the inset-B of Fig. 6. This linear tendency is a proof for the transfer of nearly same amount of NHDACx for each layer.
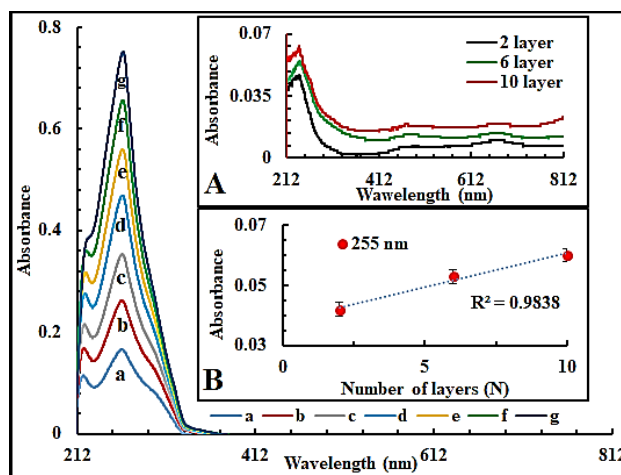

Fig. 6. UV–Vis spectra of the NHDACx in chloroform solution at different concentrations. Inset: A the NHDACx LB film on quartz glass substrate B linear increase of absorbance as a function of layer number (color online)

3.3. Calculation of refractive index and thickness of NHDACx thin film

The SPR curves of NHDACx LB thin films were fitted to determine the refractive index and thickness of these films. The fitted data were fixed with Winspall software which developed by Wolfgang Knoll Team. Refractive index and the film thickness values of NHDACx LB films at different layers were presented in Table 1. These values of NHDACx LB thin film indicate rising due to the increase of numbers' layers. The obtained values of these physical parameters are in good agreement with the literature [9]. From the SPR experimental and theoretical calculation results, it can be seen that the deposition of NHDACx monolayers onto the gold coated glass substrate was carried out successfully.

Fig. 7 displays the experimentally showed and theoretically fitted SPR curves for the bare (uncoated) gold film and coated with 6 monolayers of NHDACx. Similar processes were fixed for 2 and 10 layers as expected for this system.

As expected for this system, the thickness of NHDACx LB films increases linearly with the number of layers, and this linearship is given in Fig. 8. Similar linearship was observed in previous studies of optical characterizations [19, 20].
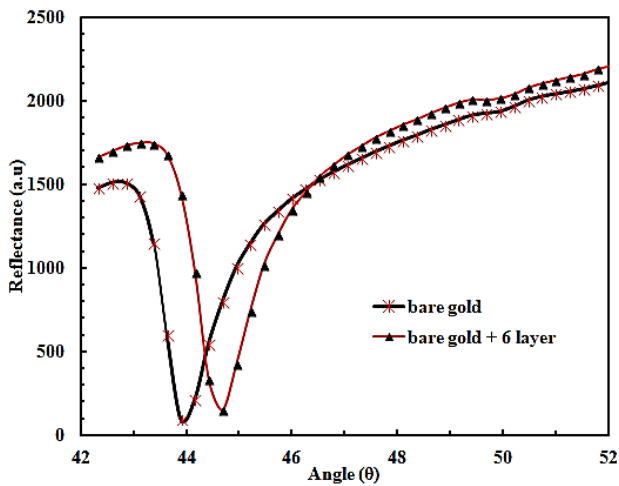
Fig. 7. Complete measured (dots) and fitted (lines) SPR curves for bare gold surface and 6 layer NHDACx LB film (color online)
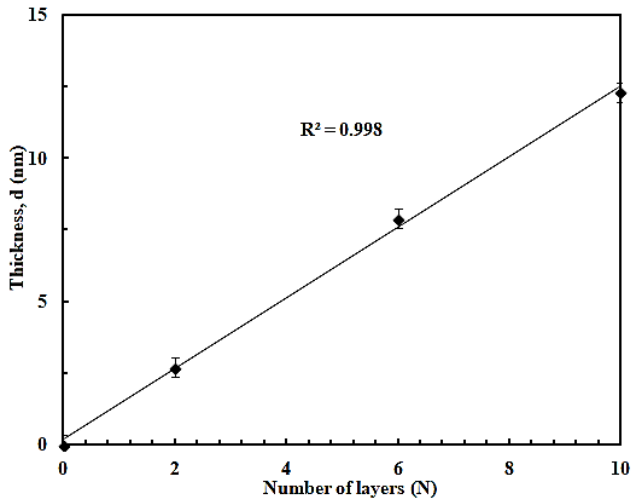

Fig. 8. Modeled layer thickness as a function of layer number for NHDACx LB layers.

Table 1. The thickness and refractive index of NHDACx thin films

	Number of LB layers	Thickness (nm)	Refractive index
NHDACx LB thin film	2 layer	2.7	1.48
	6 layer	7.9	1.53
	10 layer	12.3	1.62

3.4. Sensing properties of NHDACx LB thin film

After depositing the NHDACx LB films on the gold-coated glasses, the kinetic response of the optical sensor is measured. The response-time figures for three films (at different thickness) of NHDACx under exposure of dichloromethane, acetone, and benzene vapors are presented in Fig. 9. It can be generally mentioned that optical sensor measurements were performed in three steps (adsorption, diffusion, and desorption). Before the adsorption process started, NHDACx LB film optical sensor had exposed to fresh air for 120 s. Whenever the first interaction occurs between NHDACx optical sensor and the harmful vapor, the response of NHDACx optical sensor increases rapidly due to the surface adsorption effect (between ~120 s and 125 s). When the harmful organic vapor molecules are moved into the NHDACx thin film, the response increases gradually because of bulk diffusion effect. This interaction between host-guest molecules is called a dynamic process. In this process, adsorption and desorption occurs simultaneously. Then, the kinetic response of NHDACx optical sensor reaches the fixed value and it can be explained that the amount of the adsorbed and the desorbed molecules is approximately equal. At 240 s, the fresh air is moved to the surface of NHDACx optical sensor to observe whether the response value of optical sensor returns to the initial value or not.

Response parameter of the optical sensors in presence of the vapors is determined as $\Delta I = I_v - I_o$. I_v stands for the kinetic response of the NHDACx optical sensor in presence of the vapor and I_o related to the air. Table 2 presents the kinetic response of NHDACx optical LB thin film sensors having different thicknesses in the presence of different harmful organic vapors. The kinetic response of the optical sensor with 7.9 nm thickness of NHDACx is higher than that of the other optical sensors. These results can be interpreted that the sample with optimum thickness of NHDACx LB thin film gives rise to higher response.
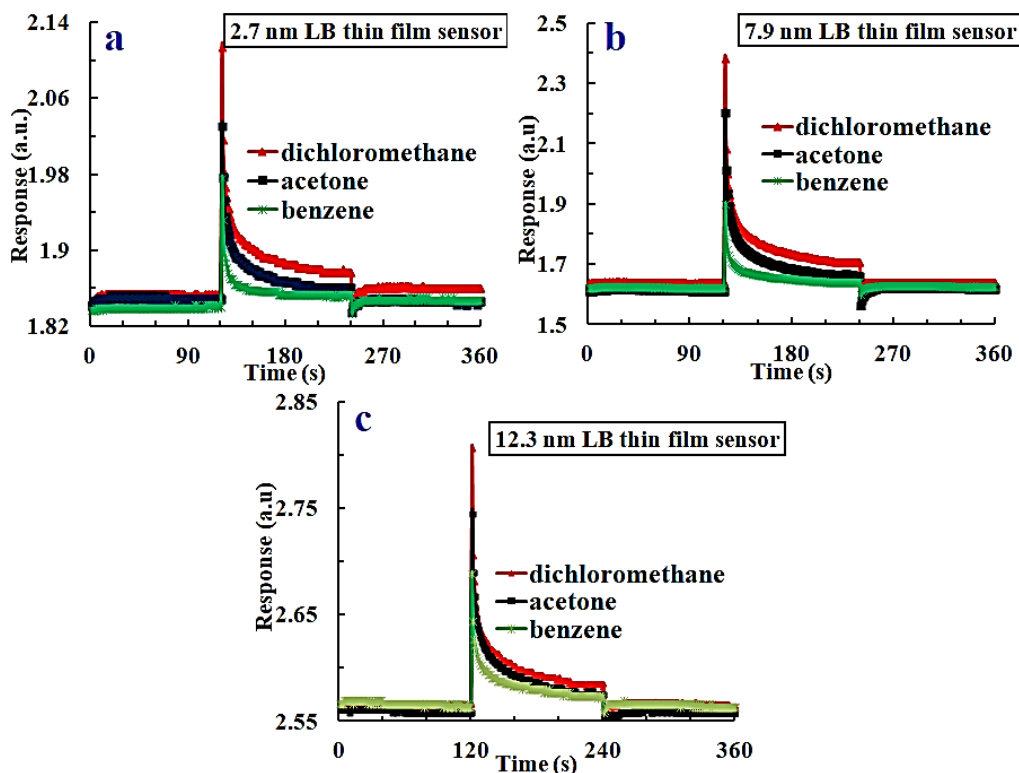
Fig. 9. The photodetector response of NHDACx LB film with a) 2.7 nm thickness b) 7.9 nm thickness c) 12.3 nm thickness against organic vapors (color online)

Fig. 10 displays the kinetic response of the optical sensor with 7.9 nm thickness of NHDACx for benzene, acetone and dichloromethane with different concentration values for 2 minutes. Diluted amounts of these vapors were described as 20 %, 40 %, 60 %, 80 %, and 100 %. These organic vapors at different concentrations were exposed to the NHDACx optical sensor for 2 min in order to record the real time changes during exposure. When the concentration of the percentage increased, the kinetic response of NHDACx optical sensor increased proportionately. Consequently, the quick response, reproducible and reversible responses were observed to all harmful organic vapors used in SPR kinetic measurements.
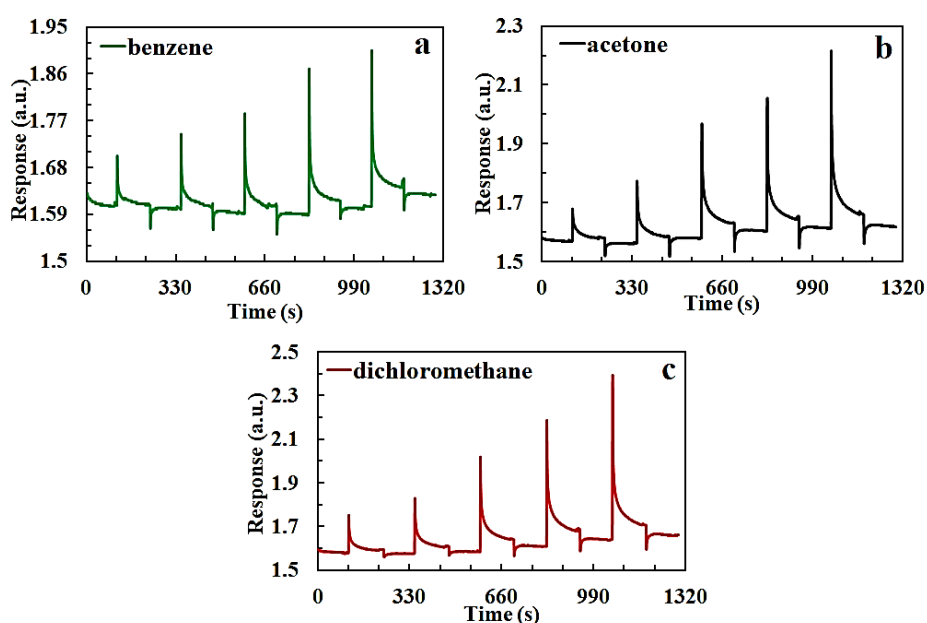

Fig. 10. The photodetector response of NHDACx optical LB thin film with 7.9 nm thickness for a) benzene b) acetone c) dichloromethane vapors at different concentrations (color online)

Also, the relationships between the change of kinetic response and the thickness of the NHDACx LB thin films for organic vapors under our study are evaluated in Fig. 11. It can be expected that increasing the thickness of the NHDACx LB thin film causes to higher shift in the kinetic response of NHDACx optical sensor. However, the obtained SPR kinetic results showed that the kinetic response of the optical sensor with 7.9 nm thickness of NHDACx is the highest against to organic vapors among other the optical sensor with different thickness (2.7 nm and 12.3 nm) of NHDACx. These results may be explained that the adsorbing vapor molecules cause to higher kinetic response.

Table 2. SPR kinetic results of NHDACx optical sensors

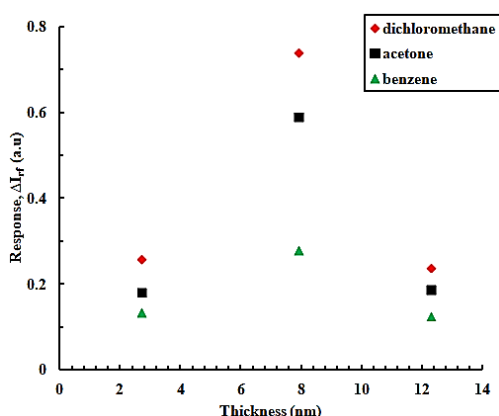| Organic vapor (saturated concentration)	Photodetector Response, ΔI (a.u)		
	2.7 nm NHDACx	7.9 nm NHDACx	12.3 nm NHDACx
Dichloromethane	0.258	0.739	0.239
Acetone	0.181	0.589	0.186
Benzene	0.135	0.278	0.125

Fig. 11. Response-thickness diagram for NHDACx based optical sensor under exposure of dichloromethane, acetone, and benzene at saturated concentration (color online)
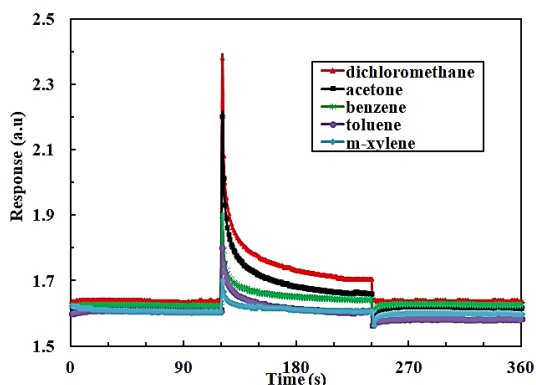

Fig. 12. The photodetector response of NHDACx optical LB thin film with 7.9 nm thickness for different five vapors (color online)

The shifts in the photodetector response (ΔI) were found to increase in the order dichloromethane > acetone > benzene for the NHDACx LB thin films with 2.7 nm, 7.9 nm, and 12.3 nm thicknesses. These SPR kinetic results can be explained in terms of the physical properties of organic vapors such as molar volume, and vapor pressure. The values of molar volume are known as dichloromethane (64.10 cm^3 mol^{-1}) < acetone (74.00 cm^3 mol^{-1}) < benzene (86.36 cm^3 mol^{-1}). While the other organic vapor molecules can difficulty penetrate into NHDACX thin film, dichloromethane molecules can easily diffusion into the same film because of its low molar volume. Similar relationship can also be observed with the effect of vapor pressure at room temperature. The values of the vapor pressures are ordered as dichloromethane (0.465 bar) > acetone (0.306 bar) > benzene (0.100 bar). As a result, dichloromethane molecules, due to its low molar volume and high vapor pressure, are more mobile than other vapor molecules and can diffuse with ease into the NHDACX LB thin film. Although, in the literature, the detection techniques used are different, chemical sensors show the largest sensitivity against dichloromethane vapor [21, 22]. Also, in this study, the photodetector response of NHDACx optical LB thin film with 7.9 nm thickness for different five vapors (dichloromethane, acetone, benzene, toluene and m-xylene) was reported and given in Fig. 12. From this graph, the lowest response value was observed for m-xylene. The m-xylene vapor is the biggest of molar volume (122 cm^3 mol^{-1}) among vapors used in this work. Therefore, the m-xylene molecules can diffuse more difficult than other vapor molecules into the NHDACX LB thin film.

4. Conclusion

This study indicated that NHDACx materials could be easily deposited onto quartz/gold-coated glass substrates *via* the LB thin film deposition technique, thus preparing an optical sensing element. The UV-Vis results and SPR curves were evaluated to determine the excellence of NHDACx LB thin film deposition. Linear relationships obtained between the number of layers and the SPR angle/absorbance indicated that highly uniform NHDACx LB films could be produced for use within an optical chemical sensor chip. The experimental SPR data were also fitted to determine some optical properties of the NHDACx films. The thickness per monolayer of NHDACx LB films was determined as 1.29 ± 0.06 nm, and 1.54 ± 0.07 for the refractive index of NHDACx materials. Vapor sensing properties of these LB films against three VOCs (dichloromethane, acetone, benzene, toluene and m-xylene) were investigated using the SPR technique. The SPR kinetic gas measurements were carried out for three LB films of NHDACx which were prepared at different thicknesses (2.7 nm, 7.9 nm, and 12.7 nm) under exposure of dichloromethane, acetone, and benzene vapors. The results of these measurements

demonstrated that the changes in the photodetector response (ΔI) were found to increase in the order dichloromethane > acetone > benzene for the all NHDACx optical sensors prepared at diffrent thickness. The optical sensor with optimum thickness (7.9 nm) of NHDACx LB thin film gave to higher response which can be explained that the adsorbing vapor molecules cause to higher kinetic response. Consequently, calix[4]arene based NHDACX material can be developed as a sensing material and may find potential applications in the development of room temperature optical sensing devices.

Acknowledgements

References

[1] S. S. Scindia, R. B. Kamble, J. A. Kher, IEEE Sens. J. **20**(23), 14072 (2020).

[2] B. R. B. da Costa, B. S. De Martinis, Clin. Mass Spectrom. **18**, 27 (2020).

[3] J. L. Medina-Franco, F. I. Saldívar-González, Biomolecules **10**, 1566 (2020).

[4] E. Marsault, M. L. Peterson, Wiley Hoboken, New Jersey, 411 (2017).

[5] L. Eddaif, A. Shaban, J. Telegdi, Int. J. Environ. Anal. Chem. **99**(9), 824 (2019).

[6] S. Kumar, S. Chawla, M. C. Zou, J. Incl. Phenom. Macrocycl. Chem. **88**, 129 (2017).

[7] R.Pinalli, A. Pedrini, E. Dalcanale, Chem. Soc. Rev. **47**, 7006 (2018).

[8] H. J. Kim, M. H. Lee, L. Mutihac, J. Vicens, J. S. Kim, Chem. Soc. Rev. **41**, 1173 (2012).

[9] Y. Acikbas, S. Bozkurt, M. Erdogan, E. Halay, A. Sirit, R. Capan, J. Macromol. Sci. A **55**(7), 526 (2018).

[10] R. Sekiya, Y. Yamasaki, W. Tada, H. Shio, T. Haino, Cryst. Eng. Comm. **16**, 6023 (2014).

[11] I. Capan, M. Bayrakci, M. Erdogan, M. Ozmen, IEEE Sens. J. **19**(3), 838 (2019).

[12] J. L. Casas-Hinestroza, M. Bueno, E. Ibáñez, Anal. Chim. Acta. **1081**, 32 (2019).

[13] Z. Ozbek, R. Çapan, H. Goktas, S. Şen, F. G. İnce, M. E. Ozel, F. Davis, Sensor Act. B: Chem. **158**, 235 (2011).

[14] A. N. Kursunlu, Y. Acikbas, M. Ozmen, M. Erdogan, R. Capan, Analyst **142**, 3689 (2017).

[15] Y. Acikbas, S. Bozkurt, E. Halay, R. Capan, M. L. Guloglu, A. Sirit, M. Erdogan, J. Incl. Phenom. Macro. **89**, 77 (2017).

[16] S. Bozkurt, M. Yılmaz, A. Sirit, Chirality **24**, 129 (2012).

[17] E. Halay, Y. Acikbas, R. Capan, S. Bozkurt, M. Erdogan, R. Unal, Tetrahedron **75**, 2521 (2019).

[18] Y. Acikbas, G. D. Tetik, C. Ozkaya, S. Bozkurt, R. Capan, M. Erdogan, Microsc. Res. Tech. **83**(10), 1198 (2020).

[19] E. Halay, S. Bozkurt, R. Capan, M. Erdogan, R. Unal, Y. Acikbas, Res. Chem. Intermed. **46**(10), 4433 (2020).

[20] A. N. Kursunlu, Y. Acikbas, M. Ozmen, M. Erdogan, R. Capan, Colloids Surf. A Physicochem. Eng. Asp. **565**, 108 (2019).

[21] Y. Acikbas, R. Capan, M. Erdogan, L. Bulut, C. Soykan, Sens. Act. B: Chem. **241**, 1111 (2017).

[22] K. Büyükkabasakal, K., S. C. Acikbas, A. Deniz, Y. Acikbas, R. Capan, M. Erdogan, IEEE Sens. J. **19**, 9097 (2019).

_____

*Corresponding author: yaser.acikbas@usak.edu.tr